Hindawi
International Journal of Antennas and Propagation
Volume 2022, Article ID 2363224, 14 pages
https://doi.org/10.1155/2022/2363224

Research Article

Generation Mechanism and Characteristic Analysis of Dual-Frequency Pseudo-Signal Interference of the Swept-Frequency Radar

Hong-Ze Zhao, Guang-Hui Wei, Xiao-Dong Pan, Xue Du, and Xu-Xu Lyu

National Key Laboratory on Electromagnetic Environmental Effects, Shijiazhuang Campus of Army Engineering University, Shijiazhuang 050003, China

Correspondence should be addressed to Guang-Hui Wei; wei-guanghui@sohu.com

Received 27 July 2022; Revised 22 September 2022; Accepted 11 October 2022; Published 20 October 2022

Academic Editor: Amrindra Pal

In order to master the law of the pseudo-signal interference effect of dual-frequency electromagnetic radiation in typical radar equipment, a certain type of Ku-band swept-frequency ranging radar was used as the test object to carry out single-frequency continuous wave and dual-frequency continuous wave pseudo-signal interference effect experiments. Through experiments, it is found that dual-frequency electromagnetic radiation will cause "hill" and "spike" type pseudo-signal interference to the swept-frequency radar. Based on the frequency analysis of the radar receiving circuit, the interference mechanism of the dual-frequency pseudo-signal is revealed, and the morphological characteristics and distance law of the pseudo-signal are explained. The variation law of the pseudo-signal level with interference field strength is obtained. The results show that the in-band dual-frequency nonintermodulation interference is similar to the single-frequency interference, and the only difference is that the number of pseudo-signals increases; when the interference frequency difference is about 400~600 MHz, the out-of-band dual-frequency second-order intermodulation signal will cause "hill" type pseudo-signal interference, and the pseudo-signal distance is random; when the interference frequency difference is less than 5 MHz, both the dual-frequency second-order intermodulation signal and the third-order intermodulation signal will cause "spike" pseudo-signal interference inside and outside the radar operating frequency band; the pseudo-signal distance is fixed.

1. Introduction

With the rapid development of information technology, the concept of electromagnetic warfare has gradually become the focus of research in various countries [1–3]. In the future, integrated joint operations under the conditions of information technology will be widely used, and the electromagnetic space will be increasingly crowded. Intentional electromagnetic interference makes the battlefield electromagnetic environment worse, and the electromagnetic environment effect of radar equipment in the complex electromagnetic environment has become a widely studied problem [4–6]. In recent years, many scholars have carried out research on the blocking effect laws and modeling evaluation methods of typical frequency equipment (such as UAV data links, communication radios, navigation receivers, and so on) in single-frequency and multifrequency continuous wave electromagnetic radiation [7–9], revealed the damage law and blocking effect mechanism of continuous wave electromagnetic radiation, established a blocking effect assessment model for multifrequency non-intermodulation interference and multifrequency intermodulation interference of frequency-using equipment [10, 11].

The radar refers to an electromagnetic sensor that uses radio to detect and range targets, which is equivalent to the human "clairvoyance" and is widely used in military and civilian fields [12]. As typical frequency equipment, a sweep continuous wave ranging radar is vulnerable to the influence of electromagnetic radiation interference signals inside and outside the band, especially the continuous wave signal in the band. Because the form of interference signal is similar to

the form of the radar useful signal, the interference signal can form pseudo-signal interference in the radar display interface under the condition of weak interference field strength. When the interference field strength is strong, the pseudo-signal strength even exceeds the true echo signal strength, causing the radar to misjudge [13]. The authors in [14] pointed out that the single-frequency signal whose jamming frequency is located in the working frequency band of the radar can cause false alarm interference to the radar, but the target characteristics of the false alarm interference were not analyzed. The author in [15] believes that single-frequency interference can cause pseudo-signal interference on the display interface of the FM CW radar, but the above-mentioned documents do not involve radar multifrequency pseudo-signal interference. In particular, the interference frequency of multifrequency signals generates intermodulation signals under certain specific frequency combinations or intermodulation signals generated by the interaction of interference signals and useful signals. The pseudo-signal strength caused by the above signals to radar equipment even far exceeds the strength of single-frequency pseudo-signals, but related research is rarely reported.

The Ku-band CW radar antenna is small in physical size, has good portability and ranging functions, and is widely used in short-range tracking and guidance [16]. In this paper, a Ku-band scanning continuous wave ranging radar is taken as the test object, and the single frequency and dual-frequency continuous wave electromagnetic radiation pseudo-signal interference effect tests are carried out in and out of the radar operating frequency band. Through experiments, the law of the dual-frequency pseudo-signal interference effect was obtained, and the mechanism and imaging mechanism of the dual-frequency pseudo-signal interference effect were revealed. The research content of this paper is not only crucial to the evaluation of the adaptability test of the complex electromagnetic environment of equipment but also lays the technical foundation and provides the mechanism and method support for the improvement of the electromagnetic protection capability of the swept range radar, which has important theoretical significance.

2. Analysis on Interference Effect Mechanism on the Single-Frequency Continuous Wave Pseudo-Signal

In this paper, the Ku-band swept continuous wave ranging radar is selected as the tested radar. The operating frequency is $f0 \pm 100$ MHz ($f0$ is the center frequency), and the transmitting signal jumps in steps of 10 kHz/0.05 ms during a single detection cycle, with a maximum detection distance of 5000 m. The authors in [13] focused on the electromagnetic interference effect of in-band single-frequency continuous wave of the swept-frequency radar and described in detail the variation law of the true target echo level and false signal level when the tested radar equipment was interfered by in-band continuous wave. However, the detection target set in the [13] is only 4.5 m. In order to avoid the effect caused by too strong echo signals and make the test results universal, we added a 30 dB attenuator at the radar transmitting port and set the detection target to about 8.3 m. The full-band electromagnetic radiation interference effect test of the swept frequency continuous wave ranging radar was carried out. After the target echo signal is received by the tested radar, it is mixed and filtered and amplified and is collected as I/Q road data at the back-end. The I/Q path data are processed by inverse fast Fourier transform to obtain a one-dimensional distance image of the target echo. The strength of the different targets is indicated by the normalized level, while the absolute value of the peak signal level is given. The experimental results show that if the single-frequency interference frequency is located in the radar operating band, the tested radar will produce pseudo-signal interference as shown in Figure 1. Outside the radar operating frequency band, if the interference frequency is close to the first local oscillator frequency of the tested radar, a pseudo-signal interference as shown in Figure 2 will also be generated. According to the morphological characteristics of the pseudo-signals, the two pseudo-signals are named "hill" type pseudo-signal and "spike" type pseudo-signal, respectively, in this paper.

The working frequency of the swept-frequency continuous wave ranging radar is relatively high, and the working bandwidth is relatively large, and it usually undergoes at least one frequency conversion process. In order to ensure the universality of pseudo-signal analysis, this paper takes a zero-IF receiver with double frequency conversion as an example. Figure 3 shows the block diagram of the tested radar schematic structure, the radar transmitting antenna and receiving antenna are taken to be separated in order to ensure the physical isolation of the two. A local oscillator fixed frequency signal and a local oscillator sweep frequency signal are generated by the frequency synthesizer, which are amplified by the mixing filter and emitted by the transmitting antenna. The echo signal returned from the target is received by the receiving antenna. After filtering and amplifying, the echo signal is first mixed with the first local oscillator-fixed frequency signal, and the frequency of the received signal is down-converted to the intermediate frequency. After filtering and amplifying, it is mixed with the second local oscillator frequency sweep signal. Then, by filtering by using a low-pass filter, the low-frequency echo signal with time delay information is further amplified. Finally, the signal is collected and processed later, the peak signal with useful target distance information can be observed in the radar, and the radar ranging function is realized.

According to Figure 3, taking the single-frequency continuous wave signal as the interference source, based on the signal processing of the swept-frequency continuous wave ranging radar receiver circuit, the analysis is carried out in the form of a complex signal. Furthermore, we discuss

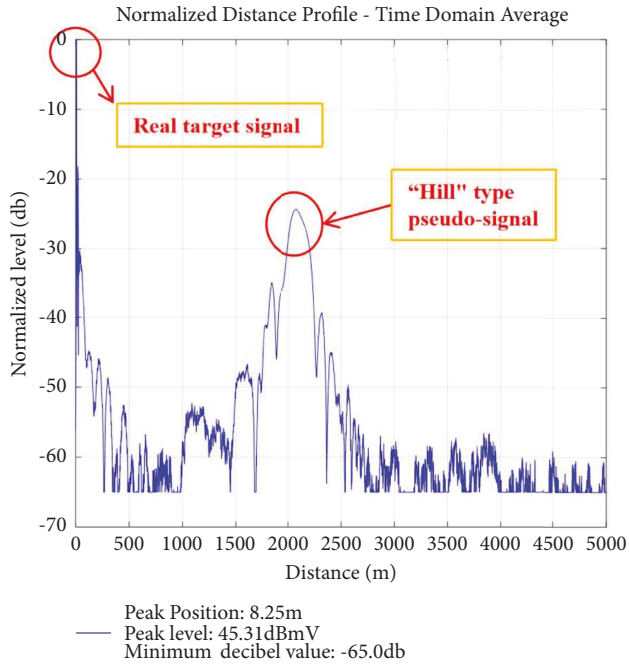

Figure 1: Schematic diagram of "hill" type pseudo-signal interference.

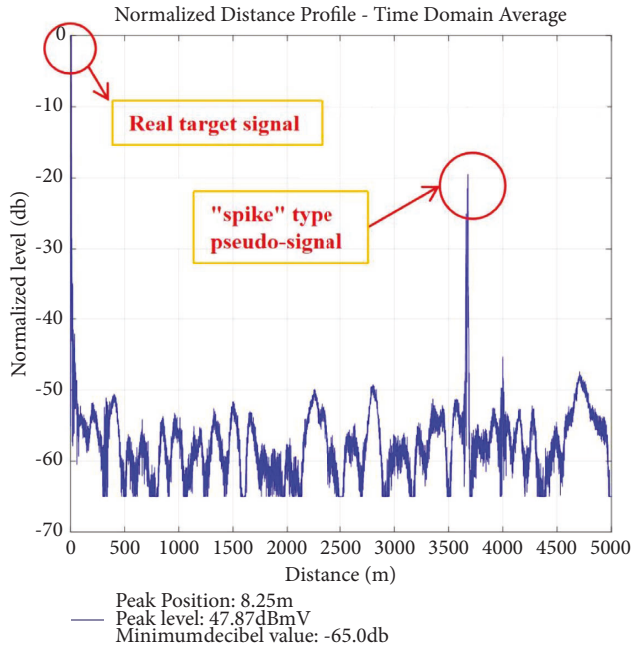

Figure 2: Schematic diagram of "spike" type pseudo-signal interference.

the imaging mechanism of real useful targets, "hill" type pseudo-signals and "spike" type pseudo-signals.

2.1. Real Target Echo Imaging Analysis. According to Figure 3, the signal sent by the transmitting antenna can be set as

$$S(t) = \sum_{i=-N/2}^{N/2} E_{si}\left\{rect\left[\frac{t - T_R/2 - (i + N/2)T_R}{T_R}\right]\exp\left[j\left(2\pi\left(f_0 + i\Delta f\right)t + \varphi_i\right)\right]\right\}. \quad (1)$$

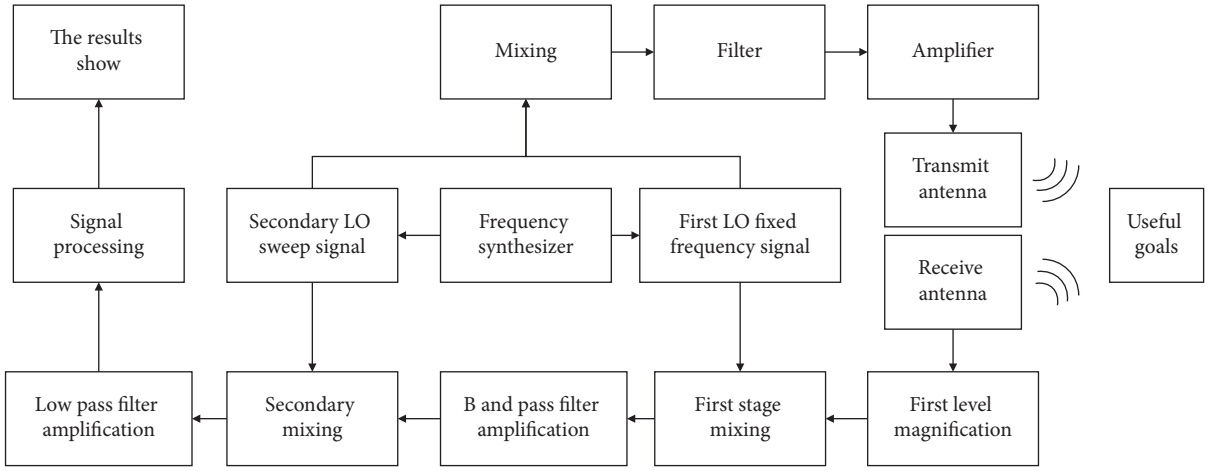

Figure 3: Sweep frequency radar principle structure block diagram.

Among them, N is the number of sweep steps, E_{si} is the signal field strength amplitude in each step, T_R is the frequency hopping time of a single step, f_0 is the center frequency of the radar operating frequency band, Δf is the sweep step, φ_i is the initial phase of each step signal, and the bandwidth of the radar operating frequency band is $2f_H$, then $N = 2f_H/\Delta f$.

Let f_a be the fixed frequency of the first local oscillator of the radar receiver, then the first local oscillator signal of the radar can be expressed as

$$u_a(t) = 2\exp\left(j2\pi f_a t\right). \tag{2}$$

Let f_b be the center frequency of the second LO of the radar receiver, then the second LO sweep signal of the radar can be expressed as

$$u_b(t) = 2\sum_{i=-N/2}^{N/2}\left\{rect\left[\frac{t - T_R/2 - (i+N/2)T_R}{T_R}\right]\exp\left[j\left(2\pi\left(f_b + i\Delta f\right)t + \varphi_i\right)\right]\right\}. \tag{3}$$

Therefore,

$$f_0 = f_a + f_b. \tag{4}$$

The real target echo signal with distance R can be expressed as

$$u_c(t) = \sum_{i=-N/2}^{N/2} A_{ci}E_{ci}\left\{rect\left[\frac{t - T_R/2 - (i+N/2)T_R - 2R/c}{T_R}\right]\exp\left[j\left(2\pi\left(f_0 + i\Delta f\right)(t - 2R/c) + \varphi_i\right)\right]\right\}. \tag{5}$$

In formula (5), c is the speed of light, and A_{ci} is the equivalent transfer function before the ith swept-frequency ladder signal field path is coupled to the nonlinear device of the radar receiver. E_{ci} is the field strength amplitude of the true target echo signal at the radar receiving antenna.

After mixing the real target echo signal with the first local oscillator signal of the radar, we obtain

$$\sum_{i=-N/2}^{N/2} A_{ci}E_{ci}\left\{rect\left[\frac{t - T_R/2 - (i+N/2)T_R - 2R/c}{T_R}\right]\exp\left[j\left(2\pi\left(f_b + i\Delta f\right)(t - 2R/c) + \varphi_i\right)\right]\right\}. \tag{6}$$

After mixing with the radar's second local oscillator signal, we obtain

$$\sum_{i=-N/2}^{N/2} A_{ci}E_{ci}\left\{rect\left[\frac{t-T_R/2-(i+N/2)T_R-2R/c}{T_R}\right]\exp\left[\mathrm{j}\left(2\pi\left(f_b+i\Delta f\right)(-2R/c)\right)\right]\right\}. \tag{7}$$

Suppose the sampling time of the sweeping ranging radar in each sweeping step is $t = t_0 + (i + N/2)T_R, t = -N/2, -N/2 + 1, \cdots, N/2$, and after sampling formula (7), the sampling sequence is obtained:

$$u_{ic}(i) = A_{ci}E_{ci}\exp\left[\mathrm{j}2\pi f_b(-2R/c)\right]\exp\left[\mathrm{j}2\pi i\Delta f(-2R/c)\right]. \tag{8}$$

The first exponential term $\exp[\mathrm{j}2\pi f_b(-2R/c)]$ in formula (8) is a constant, which only acts on the useful signal level amplitude. The second exponential term $\exp[\mathrm{j}2\pi i\Delta f(-2R/c)]$ can obtain the real target echo distance information R through fast inverse Fourier transform and threshold judgment. For the convenience of analysis, formula (8) is normalized as follows:

$$u(i) = \exp[\mathrm{j}2\pi(i+N/2)l/N]. \tag{9}$$

Among them, $l = Roun\,d(2RN\Delta f/c)$, $Roun\,d(x)$ are rounding operations. We perform the inverse fast Fourier transform operation on formula (9) and find the modulo:

$$|\bar{u}(l)| = \left\|\frac{\sin(k-l)}{\sin(k-l/N)}\right\|; k = 0, 1, 2, \cdots, N-1. \tag{10}$$

When $k = l$, then formula (10) can take the maximum value. After the threshold judgment, the real target echo distance R can be calculated by the value of k.

$$R = \frac{ck}{2N\Delta f}. \tag{11}$$

2.2. Imaging Analysis of the "Hill" Type Pseudo-Signal. Assume that the single-frequency continuous wave interference signal whose interference frequency f_1 is close to the working frequency band of the radar is

$$S_1(t) = E_1\exp\left[\mathrm{j}\left(2\pi f_1 t+\theta_1\right)\right]. \tag{12}$$

Among them, E_1 is the field strength amplitude of the interfering signal at the receiving antenna, and θ_1 is the initial phase of the interfering signal.

Then, the interference signal received before the nonlinear device of the radar receiver is

$$u_1(t) = A_1E_1\exp\left[\mathrm{j}\left(2\pi f_1 t+\theta_1\right)\right]. \tag{13}$$

Among them, A_1 is the equivalent transfer function before the interference signal field path is coupled to the nonlinear device of the radar receiver.

After the interference signal is mixed with the first local oscillator signal of the radar, we obtain

$$A_1E_1\exp\left[\mathrm{j}\left(2\pi\left(f_1-f_a\right)t+\theta_1\right)\right]. \tag{14}$$

After mixing with the radar's second local oscillator signal, we obtain

$$A_1E_1\sum_{i=-N/2}^{N/2}\left\{rect\left(\frac{t-T_R/2-(i+N/2)T_R}{T_R}\right)\exp\left[\mathrm{j}\left(2\pi\left(f_1-f_a-f_b-i\Delta f\right)t+\left(\theta_1-\varphi_i\right)\right)\right]\right\}. \tag{15}$$

Sampling formula (15), the sampling sequence can be obtained as

$$\begin{aligned} u_{i1}(i) = {} & A_1E_1\exp\left[\mathrm{j}\left(2\pi\left(f_1-f_0-f_H\right)t_0+\left(\theta_1-\varphi_i\right)\right)\right] \\ & \cdot\exp\left[\mathrm{j}2\pi\left(\left(f_1-f_0-f_H\right)T_R-\Delta f t_0\right)(i+N/2)\right] \\ & \cdot\exp\left[-\mathrm{j}2\pi\Delta f T_R(i+N/2)^2\right]. \end{aligned} \tag{16}$$

In the above formula, θ_1 and φ_i in the exponential term $\exp[\mathrm{j}(2\pi(f_1 - f_0 - f_H)t_0 + (\theta_1 - \varphi_i))]$ are both random variables, but because they do not contain the primary phase of i, the exponential term only affects the absolute level value of the pseudo-signal to a limited extent. The second exponential term $\exp[\mathrm{j}2\pi((f_1 - f_0 - f_H)T_R - \Delta f t_0)(i + N/2)]$ contains the primary phase of i, so this term determines where the pseudo-signal appears. If the frequency of the jamming signal is determined, the radar will generate a pseudo-signal at a fixed location. However, when the radar equipment measures the distance each time, the t_0 value is a random value, which will cause a random distance shift in the center position of each test pseudo-signal. The third exponential term $\exp[-\mathrm{j}2\pi\Delta f T_R(i + N/2)^2]$ contains the quadratic phase of i, which will cause the energy of the pseudo-signal to be dispersed, the waveform will be

broadened, and finally, it will appear as a "hill" type pseudo-signal. If the sweep step and frequency hopping time are not changed, the pseudo-signal waveform will not change.

In order to find out the distance of the "hill" type pseudo-signal, ignoring the influence of the third exponential term in formula (16), formula (16) is normalized:

$$u(i) = \exp\left[\mathrm{j}2\pi(i + N/2)m/N\right]. \tag{17}$$

Among them, $m = Round[N((f_1 - f_0 - f_H)T_R - \Delta f t_0)]$. Similarly, the "hill" type pseudo-signal distance R_1 is obtained:

$$R_1 = \frac{[(f_1 - f_0 - f_H)T_R - \Delta f t_0]c}{2\Delta f}. \tag{18}$$

2.3. Imaging Analysis of the "Spike" Type Pseudo-Signal. In order to distinguish it from the "hill" type pseudo-signal, the single-frequency continuous wave interference signal with the interference frequency f_2 close to the radar's first local oscillator frequency f_a is

$$S_2(t) = E_2 \exp\left[\mathrm{j}(2\pi f_2 t + \theta_2)\right]. \tag{19}$$

Among them, E_2 is the field strength amplitude of the interfering signal at the receiving antenna, and θ_2 is the initial phase of the interfering signal.

Let the interference signal received before the nonlinear device of the radar receiver be

$$u_2(t) = A_2 E_2 \exp\left[\mathrm{j}(2\pi f_2 t + \theta_2)\right]. \tag{20}$$

Among them, A_2 is the equivalent transfer function before the interference signal field path is coupled to the nonlinear device of the radar receiver.

The interference signal is intermodulated with the radar useful echo signal, that is, formula (5) is mixed with formula (20), and the intermodulation signal can be obtained:

$$\frac{1}{2}\sum_{i=-N/2}^{N/2} A_{ci}A_2E_{ci}E_2 \left\{ \begin{array}{c} rect\left[\dfrac{t - T_R/2 - (i + N/2)T_R - 2R/c}{T_R}\right] \\ \exp\left[\mathrm{j}\left(2\pi\left((f_0 + i\Delta f - f_2)t - (f_0 + i\Delta f)\dfrac{2R}{c}\right) + \varphi_i - \theta_2\right)\right] \end{array} \right\}. \tag{21}$$

When the interference frequency f_2 is close enough to the radar first local oscillator frequency f_a, the above-mentioned intermodulation signal will not be filtered out by the bandpass filter after the first local oscillator of the radar receiver. After amplification, it can be directly mixed with the second local oscillator signal of the radar to obtain

$$\frac{1}{2}\sum_{i=-N/2}^{N/2} A_{ci}A_2E_{ci}E_2 \left\{ \begin{array}{c} rect\left[\dfrac{t - T_R/2 - (i + N/2)T_R - 2R/c}{T_R}\right] \\ \exp\left[\mathrm{j}\left(2\pi\left((f_a - f_2)t - (f_0 + i\Delta f)\dfrac{2R}{c}\right) - \theta_2\right)\right] \end{array} \right\}. \tag{22}$$

Sampling formula (22), the sampling sequence can be simplified to

$$\begin{aligned} u_{i2}(i) = {} & \frac{1}{2}A_{ci}A_2E_{ci}E_2 \exp\left[\mathrm{j}\left(2\pi\left((f_a - f_2)t_0 - (f_0 - f_H)\frac{2R}{c}\right) - \theta_2\right)\right] \\ & \cdot \exp\left[\mathrm{j}2\pi\left((f_a - f_2)T_R - \Delta f\frac{2R}{c}\right)(i + N/2)\right]. \end{aligned} \tag{23}$$

It can be seen from formula (23) that the first exponential term $\exp[\mathrm{j}(2\pi((f_a - f_2)t_0 - (f_0 - f_H)2R/c) - \theta_2)]$ does not contain the phase of i, so its value is only related to the absolute level of the pseudo-signal. Because the second exponential term $\exp[\mathrm{j}2\pi((f_a - f_2)T_R - \Delta f 2R/c)(i + N/2)]$ contains the primary phase of i, if the frequency of the interference signal

and the distance to the useful target are fixed, the center position of the pseudo-signal is a fixed value. The secondary phase of i is not included in formula (23), so the energy of the pseudo-signal generated by the interference signal is concentrated, the waveform will not be scattered, and a "spike" type pseudo-signal will be generated on the radar display interface. In order to find out the distance of the "spike" type spurious-signal, formula (23) is normalized:

$$u(i) = \exp\left[j2\pi(i + N/2)n/N\right]. \quad (24)$$

Among them, $n = Roun\,d[N((f_a - f_2)T_R - \Delta f 2R/c)]$. Similarly, the "spike" type pseudo-signal distance R_2 is obtained:

$$R_2 = \frac{(f_a - f_2)T_R c}{2\Delta f} + R. \quad (25)$$

It can be seen from formula (25) that when the frequency of the interference signal is determined, the distance of the "spike" type pseudo-signal is only related to the echo distance of the useful target.

3. Dual-Frequency Pseudo-Signal Interference Sensitive Phenomenon

In order to find out the pseudo-signal interference law of the above-mentioned swept-frequency radar in the complex electromagnetic environment, the research on the pseudo-signal interference effect of dual-frequency electromagnetic radiation was carried out. The test configuration is shown in Figure 4. Two signal sources are used to generate continuous wave interference signals of different frequencies, which are injected into the radar receiving port through a combiner and a directional coupling injection module. The main parameters of the equipment are as follows: the signal generator uses ROHDE&SCHWARZ SMR20, which can generate 1~20 GHz microwave signal. The spectrum analyzer uses Ceyear company's 4204 G, and the frequency range is 9 kHz~44 GHz. The target antenna uses BBHA 9120D type dual ridge broadband horn antenna, a frequency range of 1~18 GHz, and a gain of 6.3~18 dBi. In addition, the injection coupling module with monitoring function was developed by our team.

3.1. In-Band Dual-Frequency "Hill" Type Pseudo-Signal Interference Phenomenon. When the interference frequencies of the dual-frequency CW signal are randomly combined and all are located in the single-frequency pseudo-signal interference frequency band of the radar under test, the interference characteristics are basically the same as those of the single-frequency continuous wave pseudo-signal interference. The only difference is that the radar display interface generates two "hill" type pseudo-signals, and the center positions of the pseudo-signals are randomly generated.

3.2. Out-of-Band Dual-Frequency "Hill" Type Pseudo-Signal Interference Phenomenon. In the dual-frequency electromagnetic radiation test, it is found that if the frequency combination of the dual-frequency interference is changed so that the frequency difference between the dual frequency is about 450 MHz~550 MHz, it will still cause "hill" type pseudo-signal interference to the radar. Taking the jamming frequency as $f_0 - 300$ MHz and $f_0 + 300$ MHz as an example, any single-frequency jamming signal will not cause pseudo-signal interference to the tested radar equipment, but when two jamming signals irradiate the radar at the same time, the radar display interface will be displayed. It produces a "hill" type spurious signal interference similar to Figure 1.

For this new "hill" type pseudo-signal interference sensitive phenomenon, it cannot be explained by the non-intermodulation superposition mechanism. It is necessary to explore the essential cause of this pseudo-signal interference effect from the perspective of intermodulation.

3.3. Dual-Frequency "Spike" Type Pseudo-Interference Phenomenon. On the basis of the above experiments, we continue to change the frequency difference combination of the dual-frequency interference frequencies. The test found that no matter the interference frequency is in the band or out of the band of the tested radar equipment, when the frequency difference of the dual-frequency interference is less than 5 MHz, the "spike" type pseudo-signal interference similar to Figure 2 will be caused to the tested radar equipment. The shape of the "spike" pseudo-signal is much narrower than that of the "hill" type pseudo-signal, similar to the real target signal, and the interference level of the "spike" type pseudo-signal is much higher than that of the "hill" pseudo-signal. Even when the interference field strength is low, the pseudo-signal level value has exceeded the real echo signal level value, causing the radar equipment to misjudge. This interference phenomenon deserves attention. At the same time, by changing the intensity of the dual-frequency interference signal, it is found that the "spike" type pseudo-signal is sometimes single and sometimes two. It is necessary to find out the reason for this phenomenon.

4. Generation Mechanism of Dual-Frequency Pseudo-Signal Interference

In order to further explain the imaging mechanism of the above-mentioned dual-frequency pseudo-signal, combined with the working principle and structural block diagram of the tested radar equipment, we assume the first case: the receiving antenna receives the out-of-band dual-frequency interference signal with frequencies of f_1 and f_2, and we let $f_b - f_H < f_2 - f_1 < f_b + f_H$; we suppose the second case: the receiving antenna receives interference signals with frequencies of f_3 and f_4 so that $f_4 - f_3$ is smaller than the filtering range of the low-pass filter of the tested radar. The frequency of each component of the output signal after the above-mentioned interference signal enters each structure of the tested swept-frequency radar is shown in Table 1. In Table 1, ignoring the effects of components above the third order, the frequency components shown in the table can only be output when the frequency of the interference signal is not far from the operating frequency of the radar under

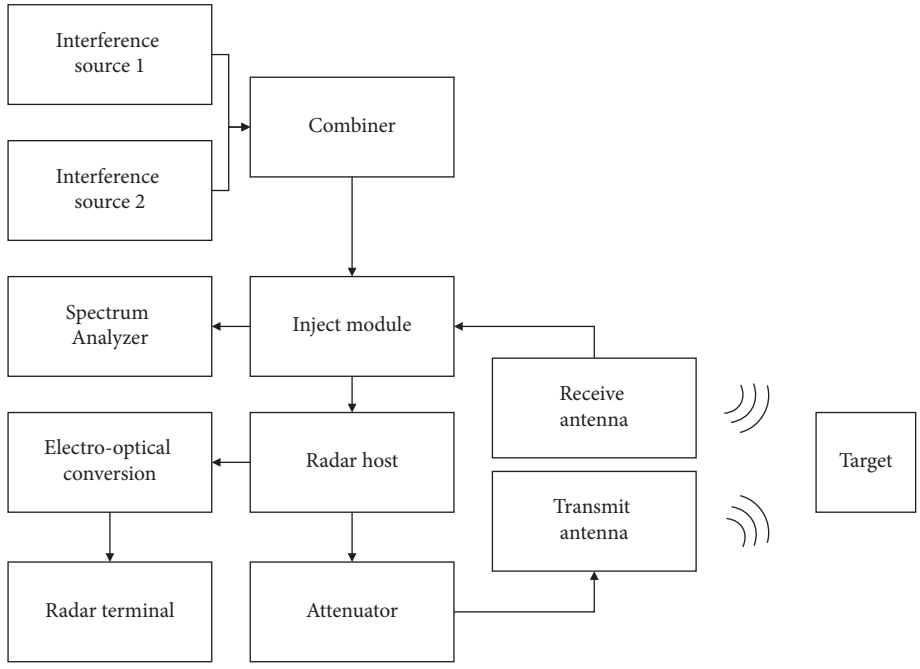

Figure 4: Configuration diagram of the dual-frequency continuous wave pseudo-signal interference test.

Table 1: After the dual-frequency interference signal enters each structure of the swept-frequency radar, the output component frequency.

Structure	Frequency	
Antenna reception	F_0, f_1, f_2	F_0, f_3, f_4
First level amplification	$F_0, f_1, f_2, F_0 \pm f_1, F_0 \pm f_2, f_2 \pm f_1, F_0 \pm (f_2 - f_1)$	$F_0, f_3, f_4, F_0 \pm f_3, F_0 \pm f_4, f_4 \pm f_3, F_0 \pm (f_4 - f_3)$
Primary mixing (f_a)	$F_0, f_1, f_2, F_0 \pm f_1, F_0 \pm f_2, f_2 \pm f_1, F_0 \pm (f_2 - f_1)$, $F_0 \pm f_a, f_1 \pm f_a, f_2 \pm f_a, F_0 \pm f_1 \pm f_a$, $F_0 \pm f_2 \pm f_a, f_2 \pm f_1 \pm f_a, F_0 \pm (f_2 - f_1) \pm f_a$	$F_0, f_3, f_4, F_0 \pm f_3, F_0 \pm f_4, f_4 \pm f_3, F_0 \pm (f_4 - f_3)$, $F_0 \pm f_a, f_3 \pm f_a, f_4 \pm f_a, F_0 \pm f_3 \pm f_a, F_0 \pm f_4 \pm f_a$, $f_4 \pm f_3 \pm f_a, F_0 \pm (f_4 - f_3) \pm f_a$
Bandpass filtering ($f_b \pm f_H$)	$F_0 - f_a, f_2 - f_1,$	$F_0 - f_a, f_3 - f_a, f_4 - f_a, F_0 \pm (f_4 - f_3) - f_a$
Secondary mixing (F_b)	$F_0 - f_a, f_2 - f_1, F_0 - f_a \pm F_b, f_2 - f_1 \pm F_b$, $F_0 - f_a \pm (f_2 - f_1)$	$F_0 - f_a, f_3 - f_a, f_4 - f_a, F_0 \pm (f_4 - f_3) - f_a, F_0 - f_a \pm F_b$, $f_3 - f_a \pm F_b, f_4 - f_a \pm F_b, F_0 \pm (f_4 - f_3) - f_a \pm F_b$, $f_4 \pm f_3, F_0 \pm f_3, F_0 \pm f_4$
Low pass filtering	$F_0 - f_a - F_b$ (real target echo signal) $f_2 - f_1 - F_b$ (second order intermodulation "hill" type pseudo-signal)	$F_0 - f_a - F_b$ (real target echo signal) $F_0 \pm (f_4 - f_3) - f_a - F_b$ (third-order intermodulation "spike" type pseudo-signal) $f_4 - f_3$ (second order intermodulation "spike" type pseudo-signal) $f_3 - f_a - F_b$ (first-order "hill" type pseudo-signal) $f_4 - f_a - F_b$ (first-order "hill" type pseudo-signal)

test. Among them, the working frequency of radar is set as F_0, and we set $f_{io} = f_0 + i\Delta f, i = -N/2, -N/2+1, \cdots, N/2-1, N/2$, then $F_0 = \left\{f_{-N/20}, f_{(-N/2+1)0}, \cdots, f_{(N/2-1)0}, f_{N/20}\right\}$. We set the second LO sweep frequency of the radar as F_b, set $f_{ib} = f_b + i\Delta f, i = -N/2, -N/2+1, \cdots, N/2-1, N/2$, then $F_b = \left\{f_{-N/2b}, f_{(-N/2+1)b}, \cdots, f_{(N/2-1)b}, f_{N/2b}\right\}$.

In Table 1, when f_3 and f_4 fall into the single-frequency "hill" type pseudo-signal interference sensitive frequency band, the first-order "hill" type pseudo-signal will be generated. From Table 1, it can be seen that the essential reason for the out-of-band dual-frequency "hill" type pseudo-signal interference is that the second-order intermodulation signal $f_2 - f_1$ is generated at the first-stage amplification of the radar receiver, and this signal can pass through the first local oscillator smoothly, band-pass filter, thereby causing interference to the radar. The essential reason for the generation of dual-frequency "spike" type pseudo-signal interference is the third-order

intermodulation signal $F_0 \pm (f_4 - f_3)$ generated at the first-stage amplification of the radar receiver, and because the frequency is similar to the radar echo signal, it can smoothly pass through all levels of filtering and can finally form a third-order intermodulation "spike" type pseudo-signal $F_0 \pm (f_4 - f_3) - f_a - F_b$ with real target echo information; at the rear end of the radar, the second-order intermodulation signal $f_4 - f_3$ generated at second-order mixing can also pass through the low-pass filter at the back end, thereby causing second-order intermodulation "spike" type spurious signal interference to the radar.

In order to explore the morphological characteristics of radar dual-frequency pseudo-signal interference, by combining equations (12) and (19), the interference signals of the interference frequencies f_1, f_2, f_3, and f_4 in Table 1 can be set as

$$\begin{cases} S_1(t) = E_1 \exp\left[\mathrm{j}\left(2\pi f_1 t + \theta_1\right)\right] \\ S_2(t) = E_2 \exp\left[\mathrm{j}\left(2\pi f_2 t + \theta_2\right)\right] \\ S_3(t) = E_3 \exp\left[\mathrm{j}\left(2\pi f_3 t + \theta_3\right)\right] \\ S_4(t) = E_4 \exp\left[\mathrm{j}\left(2\pi f_4 t + \theta_4\right)\right] \end{cases}. \tag{26}$$

Then, the interference signal received before the nonlinear device of the radar receiver can be expressed as

$$\begin{cases} u_1(t) = A_1 E_1 \exp\left[\mathrm{j}\left(2\pi f_1 t + \theta_1\right)\right] \\ u_2(t) = A_2 E_2 \exp\left[\mathrm{j}\left(2\pi f_2 t + \theta_2\right)\right] \\ u_3(t) = A_3 E_3 \exp\left[\mathrm{j}\left(2\pi f_3 t + \theta_3\right)\right] \\ u_4(t) = A_4 E_4 \exp\left[\mathrm{j}\left(2\pi f_4 t + \theta_4\right)\right] \end{cases}. \tag{27}$$

The sampling sequence of the out-of-band second-order intermodulation "hill" type pseudo-signal is

$$\begin{aligned} u_1(t)u_2(t)u_b(t) \longrightarrow{}& \frac{1}{2}A_1A_2E_1E_2 \exp\left[\mathrm{j}\left(2\pi\left(f_2 - f_1 - f_b - f_H\right)t_0 + \left(\theta_2 - \theta_1\right)\right)\right] \\ &\cdot \exp\left[\mathrm{j}2\pi\left(\left(f_2 - f_1 - f_b - f_H\right)T_R - \Delta f t_0\right)\left(i + \frac{N}{2}\right)\right] \exp\left[-\mathrm{j}2\pi\Delta f T_R\left(i + \frac{N}{2}\right)^2\right]. \end{aligned} \tag{28}$$

The sampling sequence of the second-order intermodulation "spike" type pseudo-signal is

$$u_1(t)u_2(t) \longrightarrow \frac{1}{2}A_3A_4E_3E_4 \exp\left[\mathrm{j}\left(2\pi\left(f_4 - f_3\right)t_0 - \left(\theta_4 - \theta_3\right)\right)\right] \exp\left[\mathrm{j}2\pi\left(f_4 - f_3\right)T_R\left(i + \frac{N}{2}\right)\right]. \tag{29}$$

The sampling sequence of the third-order intermodulation "spike" type pseudo-signal is

$$\begin{aligned} u_1(t)u_2(t)u_c(t)u_a(t)u_b(t) \longrightarrow{}& \frac{1}{4}A_3A_4A_{ci}E_3E_4E_{ci} \exp\left[\mathrm{j}\left(2\pi\left(f_4 - f_3\right)t_0 + \left(\theta_4 - \theta_3\right)\right)\right] \cdot \\ &\exp\left[\mathrm{j}2\pi\left(\left(f_4 - f_3\right)T_R - \Delta f\frac{2R}{c}\right)(i + N/2)\right] \end{aligned} \tag{30}$$

The first exponential term in formulas (28) to (30) only acts on the target signal level amplitude. Because the second

exponential term contains the primary phase of i, the target echo distance information can be obtained. The third exponential term in formula (28) contains the quadratic phase of i, which will make the pseudo-signal energy disperse, the waveform broaden, and finally appear as a "hill" type pseudo-signal. Formula (29) and formula (30) do not contain the secondary phase of i, so the energy is concentrated, and it finally appears as a "spike" type pseudo-signal.

From the aforementioned theory, the distance of the out-of-band second-order intermodulation "hill" type pseudo-signal can be obtained:

$$R_{21} = \frac{[(f_2 - f_1 - f_b - f_H)T_R - \Delta f t_0]c}{2\Delta f}, \tag{31}$$

because t_0 is a random quantity every time the radar detects, the position of the out-of-band second-order intermodulation "hill" type pseudo-signal is random.

The distance of the second-order intermodulation "spike" type pseudo-signal is as follows:

$$R_{43} = \frac{(f_4 - f_3)T_R c}{2\Delta f}. \tag{32}$$

The distance of the third-order intermodulation "spike" type pseudo-signal is as follows:

$$R_{c43} = \frac{(f_4 - f_3)T_R c}{2\Delta f} + R. \tag{33}$$

It can be obtained from formulas (32) and (33) that when the frequency difference of the interference signal is fixed, the positions of the second-order intermodulation "spike" type pseudo-signal and the third-order intermodulation "spike" type pseudo-signal are fixed. The distance between them is the real echo signal distance.

5. Test Verification

In order to verify the correctness of the above mechanism analysis, the test configuration shown in Figure 4 is used to set the frequencies of interference sources 1 and 2 as the interference signals of $f_1 = f_0 - 300MHz$ and $f_2 = f_0 + 300MHz$, and it is easy to know that the frequency difference of the interference signals is $\Delta f_{21} = 600MHz$. The interference signal is turned on under the normal working state of the tested radar, and the attenuation of 30 dB and 40 dB is set at the radar transmitting port to change the interference field strength of the dual-frequency signal. The test results are shown in Table 2. From this, the variation curve of the interference level of the out-of-band dual-frequency "hill" type pseudo-signal with the interference field strength is drawn as shown in Figure 5.

It can be obtained from Table 2 and Figure 5:

(1) When the dual-frequency interference field strength is low, the tested radar equipment works in the linear region, and the pseudo-signal level value increases approximately linearly with the increase of the interference field strength. When the interference field strength increases to the point that the tested radar equipment operates in a strong nonlinear region, the pseudo-signal level value basically does not change with the increase of the interference field strength.

(2) Changing the strength of the useful signal has almost no effect on the interference level value of the pseudo-signal. The interference level value of the pseudo-signal is only related to the field strength of the two interference signals, and the maximum value can reach about 16 dBmV. It is proved that the essence of out-of-band dual-frequency "hill" type pseudo-signal interference is out-of-band second-order intermodulation interference, which verifies the correctness of the theoretical analysis above.

(3) The center distance of the out-of-band dual-frequency second-order intermodulation "hill" type pseudo-signal is random because the random quantity t_0 is contained in formula (31).

The same as the previous test configuration, we change the interference source frequency to the interference signal of $f_1 = f_0$ and $f_2 = f_0 + 1.21MHz$, and it is easy to know that the frequency difference of the interference signal is $\Delta f_{21} = 1.21MHz$. We change the interference field strength of the dual-frequency signal, and the test results are shown in Table 3. From this, the variation curves of the interference level of the dual-frequency "spike" type pseudo-signal with the interference field strength are drawn as shown in Figures 6 and 7.

From Table 3, Figures 6 and 7, it can be obtained:

(1) Changing the useful signal strength only affects the interference level value of the third-order intermodulation "spike" type pseudo-signal. The distance values of the two pseudo-signals are fixed and remain basically unchanged. According to formula (32) and formula (33), the theoretical distance values of the two pseudo-signals can be calculated from the frequency difference of the interference signal frequency to 907.5 m and 915.8 m. The difference between the distances of the two pseudo-signals is the real echo signal distance. The experimental results prove the correctness of the theoretical analysis above.

(2) When the dual-frequency interference field strength is low, the tested radar equipment works in the linear region, and the second-order intermodulation and third-order intermodulation "spike" type pseudo-signal levels increase approximately linearly with the increase of the interference field strength; when the interference field strength continues to increase, the radar under test works in a strong nonlinear region, the level of the second-order intermodulation pseudo-signal gradually increases to the maximum value and remains constant, and the third-order intermodulation pseudo-signal level value reaches the maximum value. It gradually decreases. The reason is that the real target echo signal is suppressed in the strong nonlinear region of the radar, which

Table 2: Test results of the out-of-band dual-frequency second-order intermodulation "hill" pseudo-signal.

	Interference field strength 1 (dBV/m)	Interference field strength 2 (dBV/m)	Pseudo-signal level (dBmV)	Pseudo-signal center distance (m)
	−15	−15	3.35	2419
	−12	−12	7.93	253.4
Transmit signal attenuation	−9	−9	12.65	2920
30 dB	−6	−6	15.93	3211
	−3	−3	15.97	1154
	0	0	16.11	926.2
	−14	−14	4.17	540.7
	−11	−11	9.85	2175
Transmit signal attenuation	−8	−8	13.95	1243
40 dB	−5	−5	15.59	2432
	−2	−2	15.85	2376
	0	0	15.99	2428

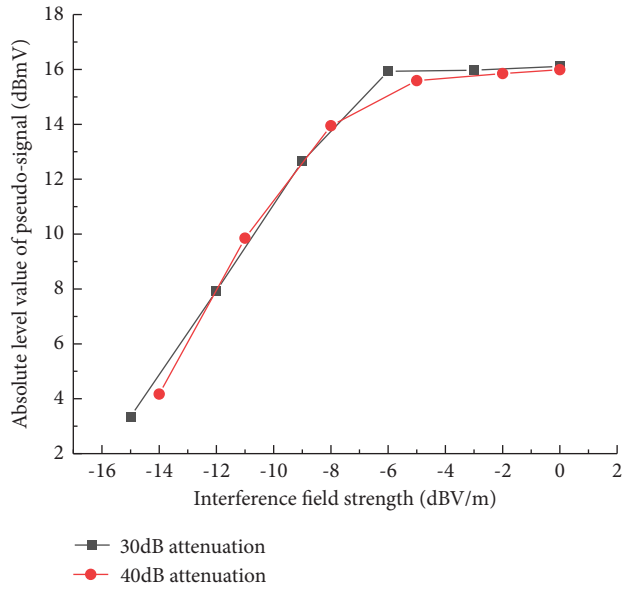

Figure 5: Variation of the two-frequency second-order intermodulation "hill" type pseudo-signal level with interference field strength.

Table 3: Two-frequency second-order intermodulation and third-order intermodulation "spike" type pseudo-signal test results.

	Interference field strength 1 (dBV/m)	Interference field strength 2 (dBV/m)	Second-order intermodulation pseudo-signal level (dBmV)	Third-order intermodulation pseudo-signal level (dBmV)	Second-order intermodulation pseudo-signal distance (m)	Third-order intermodulation pseudo-signal distance (m)	Distance difference (m)
	−59	−59	3.03	13.39	913.4	921.7	8.3
	−54	−54	7.38	20.11	917.2	925.4	8.2
	−49	−49	13.35	26.81	916.4	924.7	8.3
	−44	−44	17.62	31.36	915.7	923.9	8.2
Transmit	−39	−39	21.89	33.86	920.2	928.4	8.2
signal	−34	−34	26.04	33.09	920.2	928.4	8.2
attenuation	−29	−29	28.57	30.11	904.4	912.7	8.3
30 dB	−24	−24	28.9	27.64	906.7	914.9	8.2
	−19	−19	27.55	24.37	903.7	912.0	8.3
	−14	−14	27.66	21.1	902.9	911.2	8.3
	−9	−9	28.3	17.93	905.9	914.2	8.3
	−4	−4	28.34	14.51	909.7	917.9	8.2

Table 3: Continued.

	Interference field strength 1 (dBV/m)	Interference field strength 2 (dBV/m)	Second-order intermodulation pseudo-signal level (dBmV)	Third-order intermodulation pseudo-signal level (dBmV)	Second-order intermodulation pseudo-signal distance (m)	Third-order intermodulation pseudo-signal distance (m)	Distance difference (m)
	−59	−59	2.33	4.89	907.2	915.4	8.2
	−54	−54	8.65	10.95	904.2	912.5	8.3
	−49	−49	13.37	16.64	908.7	916.9	8.2
	−44	−44	16.7	20.42	908.7	916.9	8.2
Transmit	−39	−39	21.25	22.04	910.9	919.2	8.3
signal	−34	−34	25.17	20.11	910.9	919.2	8.3
attenuation	−29	−29	27.63	18.15	905.7	913.9	8.2
40 dB	−24	−24	28.86	15.26	906.4	914.7	8.3
	−19	−19	27.47	12.79	909.4	917.6	8.3
	−14	−14	27.67	10.86	907.2	915.4	8.2
	−9	−9	27.44	8.25	907.9	916.2	8.3
	−4	−4	28.43	6.03	908.7	916.9	8.2

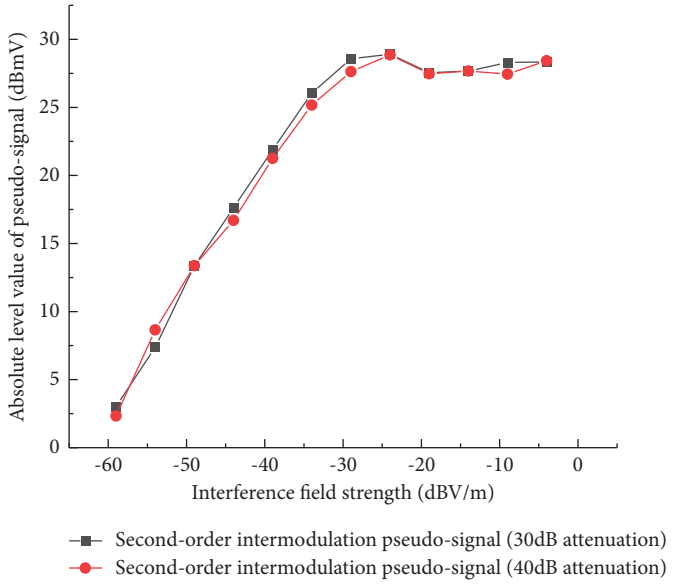

Figure 6: The second-order intermodulation "spike" type pseudo-signal level changes with the interference field strength.

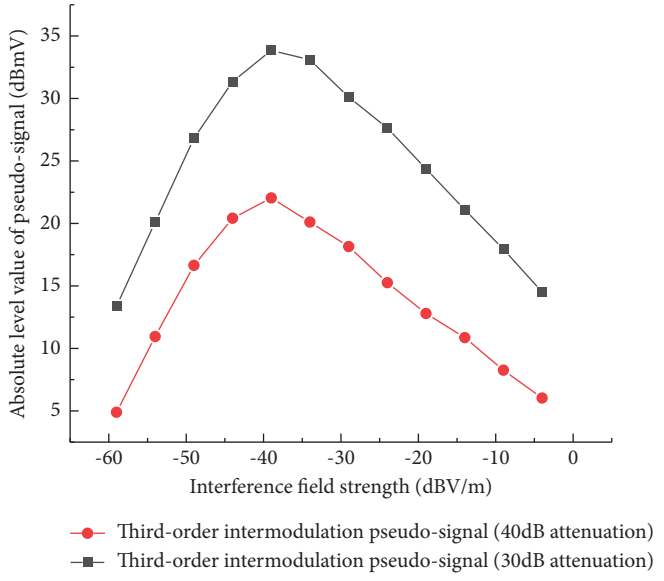

Figure 7: The third-order intermodulation "spike" type pseudo-signal level changes with the interference field strength.

affects the strength of the third-order intermodulation pseudo-signal, while the second-order intermodulation signal is not affected.

(3) When the radar works in the linear region, if the target is closer, the real echo signal is stronger, and the interference level of the third-order intermodulation pseudo-signal is higher, which is the main interference signal; if the target is far away, the real echo signal is weaker, the second-order intermodulation pseudo-signal interference level is higher, which is the main interference signal. When the radar works in the strong nonlinear region, the third-order intermodulation pseudo-signal gradually disappears, and the second-order intermodulation pseudo-signal is the main interference signal.

6. Conclusion

In this paper, on the background that the swept-frequency radar is interfered by the dual-frequency continuous wave electromagnetic radiation, the pseudo-signal interference effect test is carried out, and the pseudo-signal interference law of the swept-frequency radar under the dual-frequency continuous wave electromagnetic radiation is studied. The specific research contents and conclusions are as follows:

(1) It is revealed that the effect mechanism of out-of-band dual-frequency "hill" type pseudo-signal interference of the swept-frequency ranging radar is the second-order intermodulation radio frequency interference. The effect mechanism of dual-frequency "spike" type pseudo-signal interference is second-order intermodulation low-frequency interference and third-order intermodulation low-frequency interference. The condition for such "spike" type pseudo-signal to appear is that the frequency difference of dual-frequency interference is less than 5 MHz.

(2) The waveform shape of the "hill" type pseudo-signal is much wider than that of the "spike" type pseudo-signal because the third exponential term in the sampling sequence of the "hill" type pseudo-signal contains the quadratic phase of i, which will widen the waveform, and the energy is dispersed.

(3) The position of the second-order intermodulation "hill" type pseudo-signal is random, the second-order intermodulation "spike" type pseudo-signal interference position is fixed, and the distance is determined by the frequency difference of the dual-frequency interference. The third-order intermodulation "spike" type pseudo-signal interference position is fixed, and the distance is determined by the dual-frequency interference frequency difference and the real target distance.

(4) The maximum value of the "spike" type pseudo-signal interference level is much larger than the maximum value of the "hill" type pseudo-signal interference level. If the detection target distance is relatively short, the protection focus should focus on the third-order intermodulation pseudo-signal interference; if the interference field strength is strong, the protection focus should focus on the second-order intermodulation pseudo-signal interference.

Data Availability

The experimental data used to support the findings of this study are available from the corresponding author upon request.

Conflicts of Interest

The authors declare that they have no conflicts of interest regarding the publication of this paper.

Acknowledgments

This work was supported by the National Science Foundation of Key National Defense Basic Research Projects (41409030301) and the Key Laboratory Fund Project (6142205200301).

References

[1] T. Xu, Y. Z. Chen, Y. M. Wang, and M. Zhao, "Research on in–band con-tinuous wave electromagnetic interference effect of UAV data link[J]," *Transactions of Beijing Institute of Technology*, vol. 41, no. 10, pp. 1084–1094, 2021.

[2] S. H. Liu, Z. C. Wu, and X. J. Zhang, "Effect of electromagnetic environment and its development trend," *National Defense Technology*, vol. 31, no. 01, pp. 1–6, 2008.

[3] G. Z. Sun, S. H. Liu, and J. P. Chen, "The influence on information-based war of battle field electromagnetic environment effects [J]," *Military Operations Research and Systems Engineering*, vol. 20, no. 3, pp. 43–47, 2006.

[4] G. H. Wei, X. D. Pan, and H. J. Wan, *Feature and Mechanism of Electromagnetic Radiation Effects for Equipment*, pp. 196–198, National Defense Industry Press, Beijing, 2018.

[5] X. Lyu, G. Wei, X. Lu, H. Wan, and X. Du, "Feasibility and error analysis of using fiber Optic Temperature Measurement device to evaluate the electromagnetic Safety of Hot Bridge Wire EEDs," *Sensors*, vol. 22, no. 9, p. 3505, 2022.

[6] E. K. Mao, T. Long, and Y. Q. Han, "Digital signal processing of stepped frequency radar," *Acta Aeronautica et Astronautica Sinica*, vol. 22, no. S1, pp. 16–25, 2001.

[7] D. X. Zhang, Y. Z. Chen, and E. W. Cheng, "Effects of electromagnetic interference (EMI) on information link of UAV," *Transactions of Beijing Institute of Technology*, vol. 39, no. 7, pp. 756–762, 2019.

[8] Y. P. Wang, G. H. Wei, and W. Li, "Mechanism modeling and verification of receiver with in-band dual-frequency blocking jamming," *Transactions of Beijing Institute of Technology*, vol. 38, no. 7, pp. 709–714, 2018.

[9] G. H. Wei, J. Y. Zheng, and H. Z. Zhao, "Modeling and evaluating method of second-order intermodulation LF blocking effect for spectrum-dependent equipment," *Transactions of Beijing Institute of Technology*, vol. 41, no. 10, pp. 1095–1102, 2021.

[10] H. Z. Zhao, G. H. Wei, X. D. Pan, X. F. Lu, X. Du, and Z. K. Zhao, "Prediction method of multi-frequency non-

intermodulation electromagnetic radiation blocking effect of BeiDou navigation receiver," *AIP Advances*, vol. 12, no. 6, Article ID 065121, 2022.

[11] H. Z. Zhao, G. H. Wei, and X. Du, "Analysis of third-order intermodulation blocking effect for satellite navigation receiver[J]," *Systems Engineering and Electronics*, vol. 44, no. 04, pp. 1336–1342, 2020.

[12] G. Ding, *Study on Analysis of Electromagnetic Radiation Field Strength from Ship-Borne High Power Radar and Improvement technology*, Nanjing University of Technology, Nanjing, China, 2014.

[13] X. Du, G. H. Wei, H. Z. Zhao, and X Pan, "Research on continuous wave electromagnetic effect in swept frequency radar," *Mathematical Problems in Engineering*, vol. 2021, no. 4862451, pp. 2021–10, 2021.

[14] K. Zhao, G. H. Wei, and X. D. Pan, "Interference laws of single frequency electromagnetic radiation to radar," *Systems Engineering and Electronics*, vol. 43, no. 2, pp. 363–368, 2021.

[15] F. H. Xu, *The Impact on Target Detection of High Frequency Radar as System's Nonlinearity*, Harbin Institute of Technology, Harbin, 2010.

[16] H. Z. Zhao, G. H. Wei, X. D. Pan, X. Du, and X. X. Lyu, "Pseudo-signal interference Regularity of single-frequency electromagnetic radiation to stepped-frequency radar," *Electronics*, vol. 11, no. 17, p. 2768, 2022.